Colloids and Surfaces A: Physicochem. Eng. Aspects 482 (2015) 431–437

Contents lists available at ScienceDirect

Colloids and Surfaces A: Physicochemical and Engineering Aspects

journal homepage: www.elsevier.com/locate/colsurfa

Fabrication and optical properties of assembled gold nanoparticles film on elastomeric substrate

L. Minati[a], A. Chiappini[b], F. Benetti[c], G. Speranza[a,b,c,*], D. Zonta[d], A. Piotrowska[b,d], M. Marciniak[e], A. Vaccari[a], M. Ferrari[b,f]

[a] FBK, Sommarive str. 18, Povo, 38123 Trento, Italy
[b] CNR-IFN, CSMFO Lab., via alla Cascata 56/C, 38123, Povo, Trento, Italy
[c] Department of Industrial Engineering & Biotech Research Center, University of Trento, via delle Regole 101, 38123, Mattarello, Trento, Italy
[d] Department of Civil, Environmental and Mechanical Engineering, Trento University Via Mesiano, 77, 38123 Trento, Italy
[e] National Institute of Telecommunications, 1 Szachowa Street, 04 894 Warsaw, Poland
[f] Enrico Fermi Centre, Piazza del Viminale 1, 00184 Roma, Italy

HIGHLIGHTS

- Gold nanoparticles monolayer films were produced by water-in-oil self-assembling processes.
- Gold nanoparticles films were transferred to an elastomeric substrate by a modification of the lift-up soft lithography technique.
- The optical properties of the films were investigated as a function of the applied strain.
- Numerical simulations were performed to explain the observed behaviors.

GRAPHICAL ABSTRACT

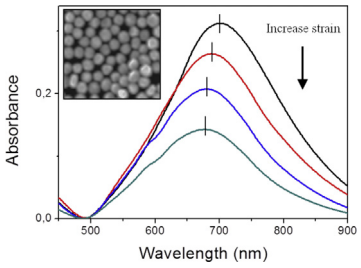

ARTICLE INFO

Article history:
Received 13 May 2015
Received in revised form 18 June 2015
Accepted 22 June 2015
Available online 25 June 2015

Keywords:
Gold nanoparticles film
Plasmonic
Soft lithography
Discrete dipole approximation

ABSTRACT

We report an easy, scalable and low cost interfacial self-assembly approach to fabricate dense metal nanoparticle monolayer films deposited on elastomeric substrate which exhibit tunable plasmonic responses to uniaxial mechanical stretching. The nanoparticle monolayers deposited on silicon substrate by water-in-oil self-assembling were quantitatively transferred to the elastic substrate by a wet lift-up soft lithography approach. By uniaxial stretching of the resulting nanoparticle film the plasmonic resonance peak experience a blue shift proportional to the applied strain. Numerical simulations were performed on the plasmon modes of the gold nanoparticles film under mechanical stress to explain the observed behaviors. Such metal nanoparticle film can be exploited in a wide range of applications in nanophotonics including strain sensors.

1. Introduction

Structural health monitoring is an important tool for maintaining and extending the lifetime of civil structures, such as bridges, buildings, tunnels and dams [1]. The interest to develop optical-based structural sensors is still present in several research groups which are exploring different techniques that can

* Corresponding author at: FBK, Sommarive str. 18, Povo, 38123 Trento, Italy. Fax: +39 461314666.
E-mail address: speranza@fbk.eu (G. Speranza).

http://dx.doi.org/10.1016/j.colsurfa.2015.06.038
0927-7757/

visualize the strain in deforming structures. Possible structures already investigated, are mechanochromic materials that show reversible color change as a function of the applied strain. Among them colloids-based photonic crystals have demonstrated some interesting properties [2]. As a further step in the framework of this research topic, we want to develop and investigate elastic structures where metal colloids constitute the template, having in mind that plasmonic properties should help in a future sensor devices [3–5].

Metallic nanoparticles cluster composed by multiple interacting elements placed in mutual proximity show intense optical fields localized in the interparticle gaps and the energy of the coupled plasmon was found to be dependent on the interparticle spacing [6,2]. The near-field coupling in interacting nanoparticles modifies the frequency of the surface plasmon oscillation of the coupled nanoparticle system with respect to that of the isolated particle. The local field intensity in the interstitial space between interacting nanoparticles can be order of magnitudes higher respect to that of the isolated nanoparticle [7,8]. In addition, nanoparticles arrays deposited of elastomeric substrates substrates can open the possibility to tune the interparticle spacing by applying a mechanical stress. The fabrication of macroarrays starting from nanoparticles building blocks represent a fundamental step in the fabrication of optical devices based on the aforementioned properties [9]. Among a wide variety of synthesis strategies, the self-assembling of nanoparticle films at the interface between two immiscible liquids represents an effective and low cost approach for the fabrication of large-area nanoparticles arrays. The self-assembly process at the interface between two immiscible liquid (typically oil and water) was firstly investigated by Pickering at the beginning of the 20th century [10]. Lately, Pieranski pointed out that the assembly of spherical particles at the oil/water interface was determined by a decrease of the total free energy of the system [11]. On the other hand, this process normally does not take place spontaneously. Reincke et al. [12] observed that by addition of a small amount of ethanol, gold nanoparticles can spontaneously form a monolayer film at the oil–water interface. The authors showed that ethanol can be adsorbed on the nanoparticles surface by removing the citrate molecules and thus inducing a decrease of the surface charge of the gold nanoparticles. In this paper we present an efficient and low cost procedure to deposit gold nanoparticles film with tunable optical properties on elastic substrate. Citrate stabilized gold nanoparticles (10 and 60 nm) were assembled into monolayers films at the water–toluene interface by using ethanol as inducers. The synthesis procedure is a variation of that proposed by Liu et al. [13] for the synthesis of monolayer nanoparticles film. Addition of consistent volume of ethanol into an aqueous gold colloid solution decreases the surface charge, inducing the migration of the nanoparticles to the water–toluene interface. A shrinking and additional package of the gold nanoparticles in the monolayer film was obtained by adding a small amount of ethanol after the nanoparticles film assembling.

The nanoparticle films deposited on silicon substrate by the water-in-oil self-assembling were quantitatively transferred to the PDMS substrate by a modified lift-off procedure. The optical properties of the gold nanoparticles films were investigated as a function of the applied strain and simulated by using the Discrete Dipole Approximation (DDA). A linear relationship was found between the applied stress and the shift of the surface Plasmon resonance band. Finally, numerical simulations were performed to investigate the dependence of the plasmon band position with the mean spacing between the nanoparticles. This work will provide an easy and reproducible approach toward the fabrication of tunable optical strain sensors based on monolayer gold colloid films deposited on PDMS.

2. Experimental

2.1. Reagents

All the reagents were purchased from Sigma–Aldrich otherwise differently indicated in the text. Spherical gold colloids (60 nm mean diameter) were purchased from Ted Pella.inc.

10 nm gold nanoparticles (NPs) were prepared by the classical citrate reduction method [14]. Briefly, 50 ml of $HAuCl_4$ water solution (1 mM) were kept to boiling. 2 ml of 1% sodium citrate water solution were added to the mixture and stirred for about 20 min until the formation of a red colored gold nanoparticle suspension.

2.2. Assembling of 10 or 60 nm gold nanoparticles film

1 ml of gold nanoparticle (AuNP) solution (10 or 60 nm) was placed in a glass beaker with 750 μl of ethanol and 1 ml of toluene was poured above the suspension. 5 ml of water were added to the biphasic mixture and the suspension was transfer in a crystallization dish. Drops of toluene with the gold nanoparticles film at the interface were formed immediately. The excess of toluene was removed by syringe until the formation of a uniform gold colloid film. 200 μl of ethanol was introduced drop by drop to form a close-package nanoparticles film. A clean glass substrates was immersed in the mixture at a certain tilted angle (10°) and the film was deposited onto one side of the substrates by slowly removing the water phase. After the adhesion of the AuNP film on the substrate the sample was washed with milli-Q water and dried in air.

2.3. Deposition of the gold colloid film on PDMS substrate

The elastomer was prepared by mixing the curing agent and base monomer at a 1:10 mass ratio. The mixture was stirred and placed in a Petri dish. The elastomer was left undisturbed for 24 h at room temperature. The obtained PDMS was cut into 35 mm × 10 mm stripes.

In a typical procedure, 10 μl of fresh toluene was placed on the gold colloid film deposited on silicon and lead to spread on the surface. Then the PDMS elastomer was placed on the Au film and a load of 2 kg was applied for 2 min. The PDMS stripe was then removed carefully from the silicon substrate and let dry in air.

2.4. Characterization

Scanning electron microscopy (SEM) images were acquired using a Zeiss Supra 40 FE SEM by an InLens detector at to 2–4 kV acceleration voltage. Atomic Force Microscopy (AFM) measurements were acquired with an NT-MDT Solver Pro in semi contact mode using epitaxially grown tips (typical curvature 1 nm, typical elastic constant 5.5 Nm^{-1}).

UV–vis absorption measurements have been performed using an UV–vis-near infrared spectrophotometer (Cary 5000) in dual beam mode. A homemade apparatus consisting of a linear stage was mounted on the spectrometer sample holder, the sample was fixed and the strain was applied in the vertical direction. All the measurements were performed with light polarized in the strain direction.

2.5. Simulation

Finite-element method COMSOL 4.3b software was used to simulate the experimental results. In the simulation, the particle clusters were delimited by a spherical perfectly matched layer (PML), which avoids spurious reflections from the particles.

The experimental values from Johnson and Christy for the dielectric function of gold were used [15]. Simulations were performed by using a gold nanoparticles (10 and 60 nm in diameter) clusters composed by 61 nanoparticles in planar hexagonal configuration. *s*-Polarized planar wave perpendicular to the nanoparticles cluster plane was used to compare the theoretical prevision with the experimental spectra.

3. Results and Discussions

3.1. Assembling of gold nanoparticles monolayer film on silicon substrate

Fig. 1 shows a schematic diagram of the mechanism for NPs assembly at a water/toluene interface using ethanol as inducer.

The driving force for the formation of a gold nanoparticles film at the interface is the decrease in the interfacial energy between water and toluene [16]. When the toluene phase was poured on the gold colloid–ethanol solution a fraction of nanoparticles migrates at the interface (Fig. 1a). When the system was perturbed by a vigorous mixing, like a fast addition of water, a close contact between the hydrophilic and oil phases occurred and the nanoparticles migrates to the interface (Fig. 1b). By carefully removing the excess of toluene by a syringe, the gold nanoparticles film shrinks and form a dense film with a strong blue color (Fig. 1c) for 10 nm gold colloid, or a golden colored film (Fig. 1d) for the 60 nm nanoparticles.

Addition of a little amount of ethanol leads to an additional shrinking of the gold colloid film.

The ethanol molecules adsorbed on the NP decreases the surface charge density of the nanoparticles and increase the contact angle of the Au NP film. This causes a migration of the gold NP to the interface between water and toluene.

Hydrophilic Au NPs can be assembled into a 2D array at liquid–liquid interfaces by tuning the contact angle of nanoparticles with the interface approaching 90°. Addition of an excess of ethanol causes a film break with the formation of floating nanoparticles aggregates. This is a consequence of the increase of the contact angle above 90°, leading to the formation of a nanoparticles multilayer. Because of the absence of hydrophobic coating the nanoparticles agglomerate at the water/toluene interface and finally precipitate.

UV–vis absorption spectroscopy analysis of 10 and 60 nm gold colloid solutions and film deposited on glass are presented in Fig. 2a and b. The spectra of the colloidal suspensions showed the classic peak at around 520–530 nm typical of isolated gold colloid in agreement with the Mie calculation [17].

UV–vis spectra of the gold nanoparticles film showed a marked red shift respect to the isolated gold colloids. This effect was attributed to the plasmon coupling of the nanoparticles induced by the interference of the dipole resonance of interacting nanoparticles in close mutual proximity [18]. The spectrum of 10 nm gold nanoparticles film reported in Fig. 2a (blue line) showed a broad plasmon band with an absorption maximum at around 700 nm. The sample deposited on silicon showed a marked yellow gold reflection as reported in Fig. 2c. Scanning electron microscopy analysis (Fig. 2d) revealed that the film was composed by a monolayer of gold nanoparticles with large domain in close package configuration separated by small voids. These holes in the films may arise from stress forces acted during the deposition of the film. The film at the interface between water and toluene was not completely flat because of the different surface tension between water and toluen. The curvature of the interface may induce a stress during the film deposition on flat silicon causing a relaxation of the film with a consequent decrease of the film package. UV–vis spectrum of 60 nm gold colloid film reported in Fig. 2b (blue line) showed a structured band with an absorption maximum at around 710 nm and a tail at 550 nm. The spectrum results very similar to that reported by Park for 1-dodecanethiol stabilized gold nanoparticles film [19]. Scanning electron microscopy analysis revealed the formation of close packaged gold nanoparticles film. The morphology was very similar to that of the 10 nm gold film indicating that in this range the NP size does not have a significant role in the self-assembling process.

3.2. Transfer of the gold nanoparticles film on PDMS substrate

The gold nanoparticles film was transferred from a silicon or glass substrate to the PDMS. The PDMS substrate was pressed onto the gold nanoparticles in presence of toluene to ensure a deep contact between the elastomer and the film. The PDMS was then carefully lifted off from the silicon substrate.

Because of the interaction between the gold nanoparticles and the PDMS surface is higher than that between gold and silicon substrate, the gold nanoparticles film were completely transferred to the elastomer. In addition, toluene is a solvent for the PDMS, and then dissolution of the surface of the elastomer could facilitate the partial embedding of the nanoparticles in the PDMS surface. This result indicates that the interaction between nanoparticles film and the silicon is lower than that between PDMS surface and gold nanoparticles.

Fig. 3a and b show the gold nanoparticles film (10 nm and 60 nm, respectively) on PDMS. Since in the deposited films the interparticle distance is in the nanoscale range, it was very difficult to experimentally determine the gap between the nanoparticle and therefore the optical spectra were modeled for various interparticle gaps. The films deposited on glass and PDMS were characterized by UV–vis spectroscopy before and after the transfer process. The UV–vis analysis of 60 nm gold nanoparticles films deposited on glass and PDMS (Fig. S1) revealed that the two spectra have very similar absorbance value. This indicates that the film deposited on PDMS is very similar to that deposited on glass.

Atomic force microscopy (see Fig. S2A) of the 60 nm gold nanoparticles deposited on PDMS revealed the morphology of the film. Phase contrast images of the edge of the monolayer film on PDMS reveals the monolayer structure with gold nanoparticles in close package configuration. This result was confirmed by the cross section analysis reported in Fig. S2B. The height and roughness of the film measured by AFM were about 73 and 11.6 nm, respectively.

3.3. Modelling of the optical properties of the gold nanoparticles films with Discrete Dipole Approximation

To model the plasmon coupling in the assembled gold nanoparticles films, we calculated the optical spectra of nanoparticles assemblies consisting of 61 spheres in a planar hexagon configuration (D6 h geometry) using the discrete dipole approximation (DDA) method. The system was composed by 10 and 60 nm gold nanoparticle cluster on PDMS substrate ($n = 1.41$). The medium surrounding the gold cluster was air. The boundary condition of the system was selected as the perfect matched layer (PML) function provided in the software package. The Johnson and Christy's values for the real and imaginary parts of gold were used. The extinction cross section was calculated as the sum of absorption and scattering cross section trough Finite Element Method (FEM) analysis under the condition of the electromagnetic field polarized in the *x*-axis parallel to the gold nanoclusters plane.

A series of simulation with different interparticle spacing were performed for both 10 and 60 nm gold nanoparticles diameters. The choice of the assembly dimensions was done on the base of simple considerations. It is known in the literature that the plasmon shift in a linear nanoparticles chain with a given spacing is dependent on the number of the nanoparticles used in the simulation (N). On

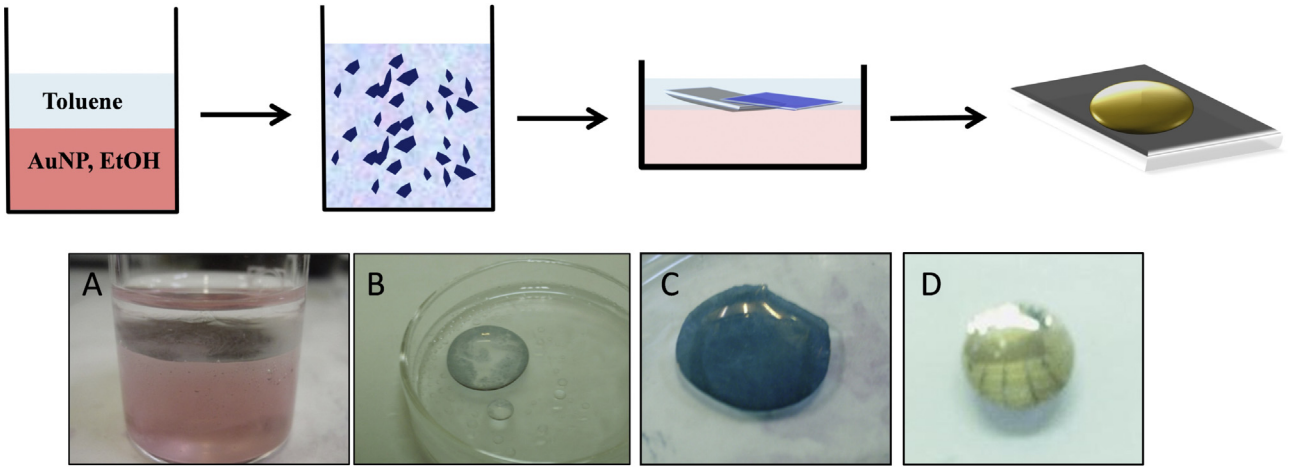

Fig. 1. Scheme of the formation and deposition of Au NP films on silicon substrate. (a) Nanoparticles suspension and toluene phase before the film formation. (b) low density Au NP film formed immediately after the addition of water to the biphasic system. (c and d) floating high density 10 and 60 nm gold colloid film.

the other hand, for $N > 8$ the nanoparticles number does not significantly change the plasmon resonance wavelength position which reaches a plateau [20]. In order to improve the simulation accuracy, instead of a simple linear 1D nanoparticles array, 2D planar clusters with 61 nanoparticles in a hexagonal conformation were used.

In this situation, the length of the cluster is $N = 9$ nanoparticles in the six principal symmetric orientation. In Fig. 4a and b the results were reported for the simulation of 10 and 60 nm gold nanoparticles film on PDMS as well as the relative experimental spectrum. The simulated curve showed a principal component at around 700 nm assigned to the dipolar resonance.

The smaller features in the range between 500 and 600 nm were attributed to higher order modes (quadrupole and octupole) that can be excited because of the low gaps between the nanoparticles. It is interesting to note that in the simulated spectrum of 60 nm nanoparticles film these last are more intense respect to the 10 nm

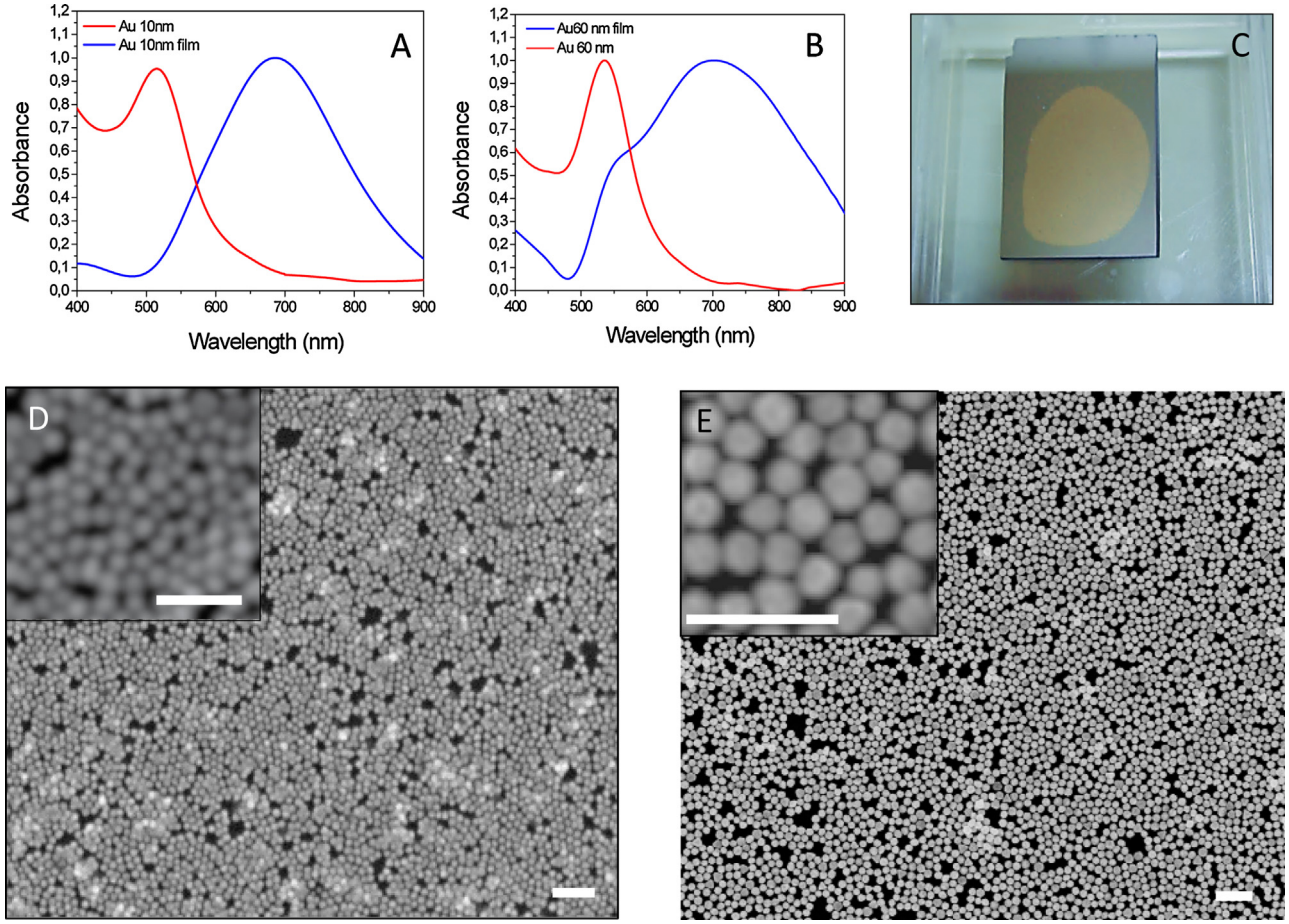

Fig. 2. (a) UV–vis absorption spectroscopy of 10 nm gold colloid (red) and AuNP film deposited on glass (blue). (b) UV–vis absorption spectroscopy of 60 nm gold colloid (red) and AuNP film deposited on glass (blue). (c) Snapshot of 60 nm gold colloid film deposited on silicon. (d and e) SEM images of 10 and 60 nm gold nanoparticles film deposited on silicon substrate. Inset. High resolution images showing the high density package of the nanoparticles. Scale bars are 50 nm for panel (d) and 300 nm for panel (e). (For interpretation of the references to color in this figure legend, the reader is referred to the web version of this article.)

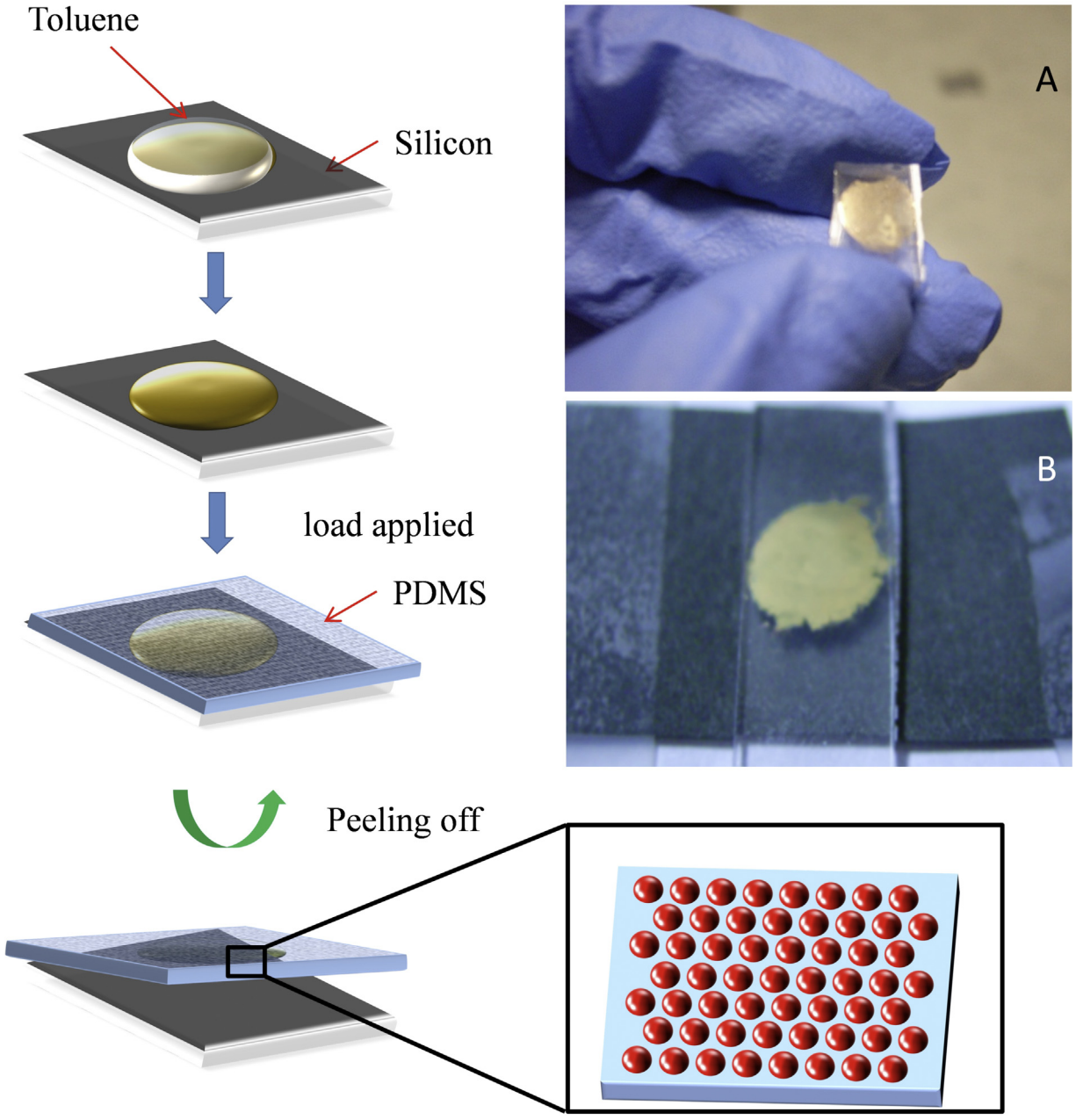

Fig. 3. Scheme of the of the gold colloid film transfer from the silicon substrate to the PDMS. (a and b) Snapshot showing the gold colloid film deposited on the PDMS surface.

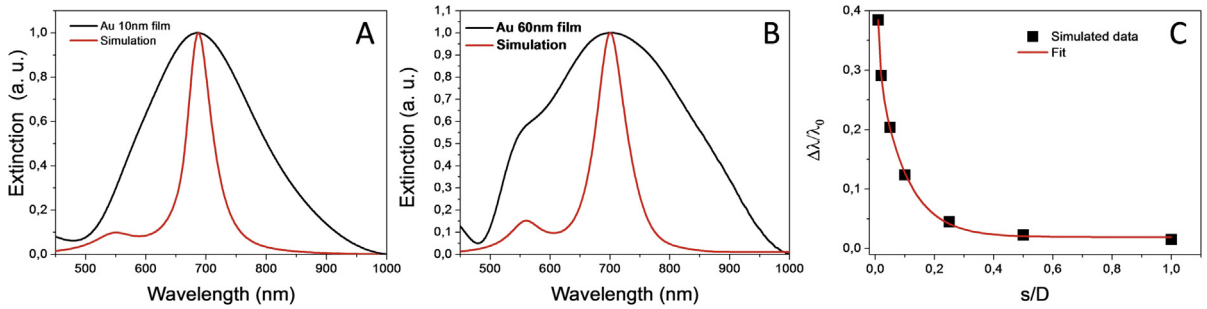

Fig. 4. Experimental and simulated extinction spectra of 10 nm (a) and 60 nm (b) gold colloid film deposited on PDMS. (c) Trend of the normalized plasmonic shift as a function of the spacing/diameter parameter.

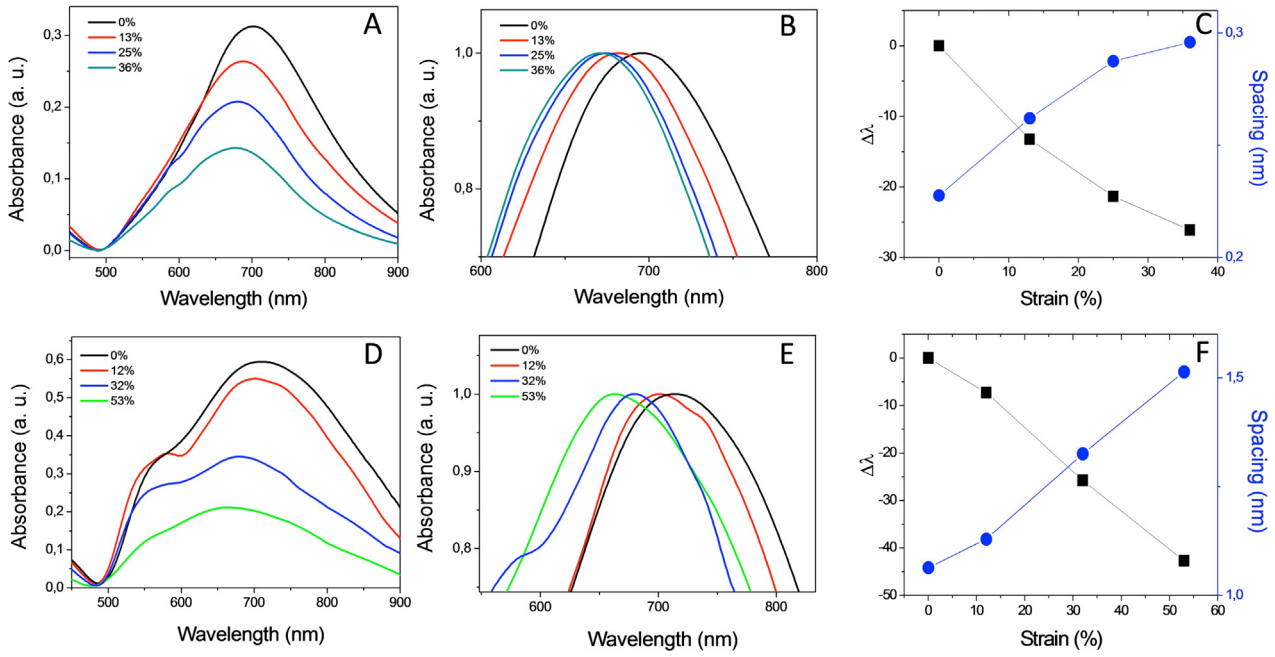

Fig. 5. Experimental extinction spectra of 10 (a) and 60 (d) gold colloid film deposited on PDMS as function of the applied strain, (b and e) are the zoomed normalized spectra of the 10 nm and 60 nm a and d images respectively. (c and f) Trend of the normalized plasmonic shift as a function of the strain (left axes) and calculated interparticle distance (right axes) for 10 and 60 nm gold nanoparticles film.

ones. This effect could be explained with the higher nanoparticles dimensions. It was observed in literature that the intensity of the high order modes increases with the nanoparticles dimension. For nanoparticles diameter higher than 100 nm quadrupolar and octupolar modes display spectral intensity comparable to that of the dipolar mode [21]. This could explain the presence of the tail at around 600 nm present on the experimental spectrum of the 60 nm gold nanoparticles film. The simulated spectra show a narrow linewidth respect to the experimental spectra. This could be a consequence of the non perfect crystalline arrangement of the gold nanoparticle in the samples. Moreover in the simulations the nanoparticles spacing are fixed while in the samples the spacing between the nanoparticles are not uniform within the sample. The presence of a spacing length distribution leads to a broadening of the plasmon resonance band associated to the gold nanoparticles film deposited on PDMS. To investigate the trend of the dipolar band position as a function of the nanoparticles spacing the approach of Jain et al. was used [22]. Fig. 4c reports the fractional plasmon shift (expressed as the simulated plasmon shift normalized by the single-particle plasmon wavelength maximum λ_0) as a function of the spacing/diameter ratio. This plot represent a "universal scale law" that is independent on the nanoparticles diameter and shape. The function showed the well know exponential decay trend and can be used to estimate the gap between the nanoparticles.

3.4. Strain test on gold nanoparticles film deposited on PDMS

A homemade apparatus was placed in the sample holder to investigate the optical properties of the samples as function of the applied strain.

The measured absorption spectra acquired with polarized light parallel to the strain direction and corrected for the PDMS absorption showed a blue shift proportional to the strains applied for both 10 and 60 nm gold nanoparticles film. This expected effect was a consequence of the increase of the interparticles distance induced by the applied strain. The absorption band shifts for 10 nm gold nanoparticles films as a function of the applied strain are shown in Fig. 5a. Fig. 5b displays a snapshot of the same spectra normalized to unity to better appreciate the plasmon shift. The absorption band shifts for 60 nm gold nanoparticles film reported in Fig. 5d and e shows a quite different behavior. Also for this sample the strain induces a blue shift of the plasmon band. However the strain causes also a visible change in the spectrum shape. This could be explained with the overlap between the dipole contribution placed at about 710 nm and the high order modes feature (500–600 nm). The blue shift in the dipolar contribution of the plasmon band maximum toward lower wavelength changed the final lineshape of the extinction spectrum. Fig. 5c and f shows the plot of the relative shift (measured as the difference of the position of plasmon peaks) as a function of the applied strain (left axes) for 10 and 60 nm gold nanoparticles film. As pointed out before, the trend result proportional to the strain indicating a progressive increase of the distance between the nanoparticles. On the right axes, the calculated mean nanoparticles distance extrapolated by using the calibration curve of Fig. 4c were reported. For 10 nm gold nanoparticles the mean interparticle gap was estimated to be around 0.24 nm for the as-deposited sample and the value increased up to 0.30 for a strain of 35%. For the 60 nm gold nanoparticles film, the mean nanoparticles gap was estimated to be around 1.1 nm for the as deposited samples and the value increased up to 1.7 with a strain of 52%. The shift of the plasmon band demonstrates that it is possible to tune the interparticle spacing at the nanometer scale by applying a macroscopic strain to the PDMS substrate. These properties can be exploited for different applications, including nano-electronics, photocatalysis, and ultrasensitive sensing.

4. Conclusion

In this paper we report a synthesis strategy to obtain tunable plasmonic material composed by self-assembled 2D gold nanoparticles films nanoparticle on transparent PDMS substrates.

The application of a macroscopic strain to the substrate induces a change in the interparticles spacing, thereby changing the optical properties of the samples. The shift in the surface plasmon resonance for the 10 and 60 nm gold nanoparticles films was explained on the basis of the plasmon coupling and simulated with the

Discrete Dipole Approximation. The possibility of obtaining optically tunable films open the way to a wide number of applications such as tunable surface enhanced Raman substrate, optical strain detectors, tunable optical filters and electronic devices.

Acknowledgments

This research is performed in the framework of MAE "Smart optical nanostructures for green photonics" (2013–2015), CNR-PAS (2014–2016) and Centro Studi e Ricerche Enrico Fermi "Strutture risonanti per la rivelazione di biomarkers precursori della sepsi" projects.

Appendix A. Supplementary data

Supplementary data associated with this article can be found, in the online version, at http://dx.doi.org/10.1016/j.colsurfa.2015.06.038

References

[1] J.M.W. Brownjohn, Structural health monitoring of civil infrastructure, Phil. Trans. R. Soc. A 365 (2007) 589–622.
[2] A. Chiappini, A. Chiasera, C. Armellini, S. Varas, A. Carpentiero, M. Mazzola, E. Moser, S. Berneschi, G.C. Righini, M. Ferrari, Sol–gel-derived photonic structures: fabrication, assessment, andapplication, J. Sol–Gel Sci. Technol. 60 (2011) 408–425.
[3] S. Zhu, C. Du, Y. Fu, Localized surface plasmon resonance-based hybrid Au–Ag nanoparticles for detection of *Staphylococcus aureus* enterotoxin B, Opt. Mater. 31 (2009) 1608.
[4] M.C. McAlpine, R.S. Friedman, C.M. Lieber, High-performance nanowire electronics and photonics and nanoscale patterning on flexible plastic substrates, Proc. IEEE 93 (2005) 1357.
[5] J. Butkus, A.P. Edwards, F.P. Quacquarelli, A.M. Adawi, Light emission enhancement using randomly distributed plasmonic nanoparticle arrays, Opt. Mater. 36 (2014) 1502.
[6] U. Kreibig, M. Vollmer, Optical Properties of Metal Clusters, Springer Series in Materials Science, Springer, Berlin, 1995.
[7] J.R. Lombardi, R.L. Birke, The theory of surface-enhanced Raman scattering, J. Chem. Phys. 136 (2012) 144704.
[8] S.K. Ghosh, T. Pal, Interparticle coupling effect on the surface plasmon resonance of gold nanoparticles: from theory to applications, Chem. Rev. 107 (2007) 4797.
[9] F. Scotognella, G. Della Valle, A.R. Srimath Kandada, D. Dorfs, M. Zavelani-Rossi, M. Conforti, K. Miszta, A. Comin, K. Korobchevskaya, G. Lanzani, L. Manna, F. Tassone, Plasmon dynamics incolloidal Cu2–xSe nanocrystals, Nano Lett. 9 (2011) 4711–4717.
[10] S.U. Pickering, Emulsions, J. Chem. Soc. Trans. 91 (1907) 2001.
[11] P. Pieranski, Two-dimensional interfacial colloidal crystals, Phys. Rev. Lett. 45 (1980) 569.
[12] F. Reincke, S.G. Hickey, W.K. Kegel, D. Vanmaekelbergh, Spontaneous assembly of a monolayer of charged gold nanocrystals at the water/oil interface, Angew Chem. Int. Ed. 43 (2004) 458.
[13] C. Liu, Y.J. Li, M.H. Wang, Y. He, E.S. Yeung, Rapid fabrication of large-area nanoparticlemonolayer films via water-induced interfacial assembly, Nanotechnology 20 (2009) 065604.
[14] G. Frens, Controlled nucleation for the regulation of the particle size in monodisperse goldsuspensions, Nat. Phys. Sci. 241 (1973) 20.
[15] P.B. Johnson, R.W. Christy, Optical constants of the noble metals, Phys. Rev. B 6 (1972) 4370.
[16] L.F. Hu, M. Chen, X. Fang, L. Wu, Oil–water interfacial self-assembly: a novel strategy for nano film and nano device fabrication, Chem. Soc. Rev. 41 (2012) 1350.
[17] G. Mie, Beiträge zur optik trüber medien, speziell kolloidaler metallösungen, Ann. Phys. 330 (1908) 377.
[18] T.J. Norman, C.D. Grant, A.M. Schwartzberg, J.Z. Zhang, Structural correlations with shifts in the extended plasma resonance of gold nanoparticle aggregates, Opt. Mater. 27 (2005) 1197.
[19] Y.K. Park, S. Park, Directing close-packing of midnanosized gold nanoparticles at a water/hexane interface, Chem. Mater. 20 (2008) 2388.
[20] Z.B. Wang, B.S. Lukyanchuk, W. Guo, S.P. Edwardson, D.J. Whitehead, L. Li, Z. Liu, K.G. Watkins, The influences of particle number on hot spots in strongly coupled metal nanoparticles chain, J. Chem. Phys. 128 (2008) 094705.
[21] J. Rodriguez-Fernandez, J. Perez-Juste, F.J.G. de Abajo, L.M. Liz-Marzan, Seeded growth of submicron Au colloids with quadrupole plasmon resonance modes, Langmuir 22 (2006) 7007.
[22] P.K. Jain, W. Huang, M.A. El-Sayed, On the universal scaling behavior of the distance decay of plasmon coupling in metal nanoparticle pairs: a plasmon ruler equation, Nano Lett. 7 (2007) 2080.